Resist and Transfer Free Patterned CVD Graphene Growth on ALD MoC_x Nano Layers

Eldad Grady[1], Chenhui Li[2], Oded Raz[2], W.M.M. Kessels[1], and Ageeth A. Bol[1]

[1] *Department of Applied Physics, Eindhoven University of Technology, Den Dolech 2, P.O. Box 513, 5600 MB Eindhoven, The Netherlands*
[2] *Institute for Photonic Integration Eindhoven University of Technology Den Dolech 2, 5612 AZ Eindhoven, the Netherlands*

Abstract

Multilayer graphene (MLG) films were grown by chemical vapour deposition (CVD) on molybdenum carbide (MoC_x) substrates. We fabricated the catalytic MoC_x films by plasma enhanced atomic layer deposition. The mechanism of graphene growth is studied and analysed for amorphous and crystalline MoC_x films. In addition, we present a complete bottom up patterned graphene growth (GG) on pre-patterned MoC_x ALD performed at $50°C$. Selective CVD GG eliminates the need to pattern or transfer the graphene film to retain its pristine, as grown, qualities. Furthermore, we fabricated MLG directly on 100 nm suspended SiN membrane. We demonstrate these qualities with characterisation of the MLG using Raman spectroscopy, and analyse the samples by scanning electron microscopy and X-ray diffraction measurements. The techniques of graphene device manufacturing demonstrated here pave the path for large scale production of graphene applications.

1 Introduction

Next generation graphene-based applications would require a resist and transfer free graphene growth in order to realise the promise of graphene for flexible electronics[1, 2], and sub 10nm nodes' interconnects[3] . Graphene based interconnects would significantly reduce the RC delay and thermal budget which is currently the bottle neck in sub 10nm transistor nodes [4, 5] due to the excellent room temperature carrier mobility and thermal conductivity. However, graphene based devices exhibit far lower carrier mobility than the theoretical predictions promise. Encapsulation of graphene with lattice matching dielectric material such as hBN shows remarkable improvement, but are still subpar [6]. The main challenges of current commercial chemical vapour deposition (CVD)

grown graphene are resist residue due to target transfer process [7, 8], and patterning of graphene, which degrade the graphene quality, resulting in the far lower carrier mobility than theoretical predictions. Known techniques include photolithography, ion beam milling [9], shadow masking [10], area selective passivation layer [11] and stencil mask [12]. Despite these tremendous efforts, the goal of a scalable, low cost, high quality patterned graphene using commercially available tools, has not been achieved. Photolithography methods leave resist residue, and ion beam etching causes broad lateral damage close to pattern area due to scattering ions [13, 14]. Patterning graphene with oxygen plasma inevitably oxides graphene edges [15], and the stencil mask poses resolution limitation . Furthermore, transfer of graphene from one substrate onto another degrades the graphene quality due to induced film compression and tension, and potential contamination between the graphene and target interfaces. A wholesome solution that avoids both the need to pattern the graphene or to transfer a pre patterned graphene onto a target, has yet to be introduced. While advancements have been made toward transfer free graphene grown on patterned Mo catalytic layer [16], resist residue on the underlying growth substrate cannot be fully removed. As defects, non uniformity and contamination will imminently translate to graphene defects, it is vital to achieve a resist free catalytic surface, in a uniform and conformal layer deposition. Atomic layer deposition (ALD) is a cyclic, broad temperature window soft deposition, with precise thickness control due to its self-limiting nature. It allows for unmatching conformal deposition on high-aspect ratio (HAR) objects. Recently, we demonstrated the plasma enhanced ALD (PEALD) of MoC_x, with excellent composition control [17]. Consequently, we presented the growth of multilayer graphene (MLG) films on these substrates, and the correlation between the catalytic substrate physical and chemical properties to the grown MLG [18]. In this work, we describe the growth mechanism of graphene on MoC_x, and compare between amorphous and highly crystalline catalytic substrates for graphene growth. Finally, we demonstrate a proof of concept for the merits of ALD based graphene growth for future interconnects (IC) in the form of low temperature patterned PEALD of MoC_x, for selective CVD growth of MLG, so that no resist residue is present between the graphene and the catalytic material interface. Additionally, we show the advantage of the ALD soft deposition on 100nm thick suspended SiN membrane. Thereafter, MLG was grown on the suspended SiN membranes to achieve suspended graphene based heterostructure without exposing the suspended MLG to wet chemicals or corrosive acids.

2 Experimental methods

MoC_x thin films have been deposited by plasma enhanced atomic layer deposition (PEALD) at various temperatures and plasma conditions, as described elsewhere [17].

PEALD was performed on 100 mm Si (100) wafers coated with 450 nm of thermally grown SiO_2. The depositions were performed in an Oxford instru-

ments FlexAL2 ALD reactor, which is equipped with an inductively coupled remote RF plasma (ICP) source (13.56 MHz) with alumina dielectric tube. MoC_x thin films have been deposited by PEALD at various temperatures and plasma conditions, with MoC_x films varying from $15\mu m$ to $30\mu m$ in thickness. MLG was grown by low-pressure CVD (LPCVD) in a quartz tube (d=50mm, l=60cm) furnace with 3 heat zones set to 1050°C. The typical base pressure when evacuated is 10^{-3} mbar. The furnace is set on cart wheels, to allow samples to be rapid annealed, as furnace temperature stabilises within 3.5 minutes after tube insertion. When moved away from the furnace, sample cooling down duration is typically 15 minutes. Carbon feedstock gas (CH_4) is fed along with Argon through a quartz inner tube of 5 mm in diameter to the sealed side of the outer tube. MoC_x films have been saturated with carbon by annealing at temperatures between $500°C$ to $800°C$ with 100 sccm CH_4 gas flow at 4 mbar pressure. Then, graphene films have been grown under similar conditions at 1100°C for 10 minutes. The samples were then promptly extracted from the furnace and allowed to cool down at ambient room temperature under Ar gas flow in the quartz tube. As shown in figure 3a photoresist (PR) ma-N 400 with 4.1 μm thickness on 90 nm SiO_2 on Si 2" wafers were used for low temperature PEALD of MoC_x film. After deposition, MoC_x was patterned by lift-off process, and rinsed in isopropyl alcohol (IPA). 100 nm and 50 nm SiN membranes were supplied by Philips Innovation Services (PInS) foundry. As shown in figure 4b MoC_x were also deposited at $300°C$ on 100 nm SiN membranes suspended on Si (5x5 mm rectangle). MLG were then grown the MoC_x films as illustrated in figure 4a. While deposition was successful for both SiN sample thicknesses, due to the brittle nature of the thinner membranes we present here results measured on the thicker 100nm based membranes. Raman spectroscopy was performed with Reinshaw InVia 514 nm laser. Film crystallinity and preferred crystal orientation was studied by Gonio x-ray diffraction. Experiments were conducted with PanAnlytical X'pert PROMRD diffractometer operated using $CuK\alpha(\lambda = 1.54A)$.

3 Characterisation and Results

This part is divided to three parts: first part deals with MLG growth mechanism in MoC_x films and comparison between amorphous and crystalline catalytic substrate. The second part demonstrate a technique for resist and transfer free patterned graphene device. In the third part we fabricate MLG on a thin suspended membrane using ALD and CVD. We show the limitation of Raman measurements on suspended membranes low thermal conductivity.

3.1 Carburisation of MoC_x

We studied the growth mechanism of graphene on MoC_x substrates, to optimise growth process for the various film compositions. The importance of saturating the catalytic MoC_x with free carbon is demonstrated and the effects of film

crystallinity on carbon precipitation to the surface during growth is shown by Raman and XRD measurements. The mechanism of graphene growth on MoC_x films is explained in this section. When we subjected the MoC_x film to direct growth at $1100°C$ for 10 minutes. SEM images show ablation on the film surface, that has a characteristic graphene Raman signature [1a]. Outside these areas, no indication of graphene growth was measured. We added then a carburisation step in order to saturate the film with carbon and examined different temperatures around the crystalline phase change temperature ($\sim 650°C$). Figure 1c indicates that ideal saturation takes place above the crystalline phase change, for MLG grown at the same growth time. After establishing an optimal carburisation temperature, we examined the ideal growth time for various MoC_x types. As seen in figure 1b, MoC_x with rich carbon content, typically low mass density and crystallinity exhibit good quality MLG growth after 10 minutes at $1100°C$. MoC_x films with higher mass density and crystallinity display no graphene growth at this time duration, but rather require a longer exposure time to CH_4 at the growth temperature of 20 minutes. Longer exposure begin to deteriorate the graphene film. We study the physical alteration for this crystalline film during the carburisation and graphene growth process, as seen in figure 2b. XRD diffraction peak typical to cubic- $MoC_{0.75}$ are dominant for the deposited film. After 2 hours carburisation at $800°C$, a transition Orthorhombic crystalline phase is noted, along with sharp graphite (101) plane diffraction peak. After 10 minutes graphene growth at $1100°C$, the orthorhombic phase crystallinity increases, while no significant change in the graphitic peak is noticed.

3.2 Patterned MLG Growth

When depositing MoC_x at $150°C$ we found resist residues on the SiO_2, due to hard baking of the photoresist at this temperature, as the thermal stability limits of the PR ($110°C$). Moreover, after the CVD growth we found random patches of MLG coverage on the exposed MoC_x, and no continuous MLG coverage. However, when the PEALD is performed at $50°C$, we could seamlessly remove the PR and no significant traces were found after lift-off. The CVD growth of graphene on these samples showed full MLG coverage with excellent uniformity, albeit a relatively high D/G peak ratio. Moreover, as can be seen in figure 2c, D and G peaks were detected throughout the exposed SiO_2 areas, but no significant 2D peak. We speculate that decomposition of the CH_4 molecules on the SiO_2 surface with PR interface residue is the reason for the carbide formation outside the patterned MoC_x areas. We have seen that a transfer free release of MLG on MoC_x membranes is a direct result of wet etching the Mo based catalyst. This observation is valid for ultra thin layers with thicknesses below 30 nm. Thicker layers ($> 50nm$) release the MLG film such that the graphene membrane is afloat on the liquid surface.

3.3 MLG Growth on Suspended Thin Film

MLG film grown on SiN membrane were characterised by Raman spectroscopy, as can be seen in 5. We measured the Raman signal at the edge of the suspended membrane where the SiN was supported by the underlying Si, and at the centre of the membrane, where the MLG was on top of $\sim$ 15nm MoC_x and 100 nm SiN. The Raman spectrum was fitted and baseline corrected due to enhanced SiN background signal. Although Raman spectroscopy is considered a non-destructive measurement, we discovered that suspended MLG/SiN membranes were highly sensitive to the Raman laser power. As figure 5c shows, when 10% power of the 20mW Laser was used, an increase in the D peak was measured, and the 2D peak was quenched in comparison to 5% power. With 50% power of the Raman's laser, we could punch a hole through the heterostructure suspended membrane [see figure 5d].

4 Discussion and Conclusions

We have demonstrated in this work the growth mechanism and conditions of MLG on PEALD MoC_x films. We compared MLG growth time on amorphous film and on a highly crystalline one. The prolonged annealing time necessary to grow graphene on crystalline film is stipulated to result from low carbon saturation during carburisation due to the dense crystal structure and the resulting low bulk precipitation of free carbon. Defects ratio of MLG on crystalline film could be explained with the transition from highly crystalline cubic-$MoC_{0.75}$ to polycrystalline orthorhombic phase, which potential creates multiple strain points in the MLG film. Therefore, growth on a amorphous carbon rich film will be much more facile and result in lower D/G peak ratios. After understanding the growth mechanism, we demonstrated the advantages of graphene growth on PEALD catalytic films. The low temperature, soft and atomic precise deposition allows for pre patterning of catalytic substrates, such that no resist residue is left on the growth surface. We demonstrated here an initial proof of concept, which showed a full film coverage with excellent uniformity. The relatively high D/G peak could be addressed by growth process optimisation, which was out of the scope of this work. We use ALD to deposit MoC_x films on brittle SiN membranes of 50 and 100 nm. The MLG growth demonstrated on 100 nm suspended membrane shows a viable fabrication route for sensor application, and graphene based resonators for a wide range of frequencies. We showed for the first time damage to a suspended heterostructure caused directly by Raman measurements. The low thermal conductivity of the SiN is likely the cause for the local damage to the suspended heterostructure, with no directly available heat sink - as oppose to the membrane edges. Building on the capabilities demonstrated here, the route for future application based on patterned graphene or suspended graphene heterostructure is clearly marked. Further steps, such as Al_2O_3 encapsulation, could be readily performed by ALD directly on the MLG without damage by a process of hydrogenation and post ALD annealing [19].

Moreover, one can combine recent developments in area selective ALD to realise a complete bottom up fabrication of the catalytic substrate resist free.

Acknowledgements

E. Grady would like to acknowledge the financial support of the Dutch Technology Foundation STW (project number 140930), which is part of the Netherlands Organisation for Scientific Research (NWO). E. Grady thanks Cristian Helvoirt, Janneke Zeegbregts, Jeroen van Gerwen and the lab technical staff for their support.

References

[1] Veronica Strong, Sergey Dubin, Maher F El-Kady, Andrew Lech, Yue Wang, Bruce H Weiller, and Richard B Kaner. Patterning and electronic tuning of laser scribed graphene for flexible all-carbon devices. *ACS nano*, 6(2):1395–1403, 2012.

[2] Rak-Hwan Kim, Myung-Ho Bae, Dae Gon Kim, Huanyu Cheng, Bong Hoon Kim, Dae-Hyeong Kim, Ming Li, Jian Wu, Frank Du, Hoon-Sik Kim, et al. Stretchable, transparent graphene interconnects for arrays of microscale inorganic light emitting diodes on rubber substrates. *Nano letters*, 11(9):3881–3886, 2011.

[3] Ning C Wang, Saurabh Sinha, Brian Cline, Chris D English, Greg Yeric, and Eric Pop. Replacing copper interconnects with graphene at a 7-nm node. In *2017 IEEE International Interconnect Technology Conference (IITC)*, pages 1–3. IEEE, 2017.

[4] Maria Politou, Xiangyu Wu, Inge Asselberghs, Antonino Contino, Bart Soree, Iuliana Radu, Cedric Huyghebaert, Zsolt Tokei, Stefan De Gendt, and Marc Heyns. Evaluation of multilayer graphene for advanced interconnects. *Microelectronic Engineering*, 167:1–5, 2017.

[5] Yuji Awano. Graphene for vlsi: Fet and interconnect applications. In *2009 IEEE International Electron Devices Meeting (IEDM)*, pages 1–4. IEEE, 2009.

[6] Shaloo Rakheja, Vachan Kumar, and Azad Naeemi. Evaluation of the potential performance of graphene nanoribbons as on-chip interconnects. *Proceedings of the IEEE*, 101(7):1740–1765, 2013.

[7] Junmo Kang, Dolly Shin, Sukang Bae, and Byung Hee Hong. Graphene transfer: key for applications. *Nanoscale*, 4(18):5527–5537, 2012.

[8] Woosuk Choi, Muhammad Arslan Shehzad, Sanghoon Park, and Yongho Seo. Influence of removing pmma residues on surface of cvd graphene using

a contact-mode atomic force microscope. *RSC Advances*, 7(12):6943–6949, 2017.

[9] Max C Lemme, David C Bell, James R Williams, Lewis A Stern, Britton WH Baugher, Pablo Jarillo-Herrero, and Charles M Marcus. Etching of graphene devices with a helium ion beam. *ACS nano*, 3(9):2674–2676, 2009.

[10] Yong Seung Kim, Kisu Joo, Sahng-Kyoon Jerng, Jae Hong Lee, Euijoon Yoon, and Seung-Hyun Chun. Direct growth of patterned graphene on sio 2 substrates without the use of catalysts or lithography. *Nanoscale*, 6(17):10100–10105, 2014.

[11] Mario Hofmann, Ya-Ping Hsieh, Allen L Hsu, and Jing Kong. Scalable, flexible and high resolution patterning of cvd graphene. *Nanoscale*, 6(1):289–292, 2014.

[12] Keong Yong, Ali Ashraf, Pilgyu Kang, and SungWoo Nam. Rapid stencil mask fabrication enabled one-step polymer-free graphene patterning and direct transfer for flexible graphene devices. *Scientific reports*, 6:24890, 2016.

[13] L Gustavo Cançado, A Jorio, EH Martins Ferreira, F Stavale, Carlos Alberto Achete, Rodrigo Barbosa Capaz, Marcus Vinicius de Oliveira Moutinho, Antonio Lombardo, TS Kulmala, and Andrea Carlo Ferrari. Quantifying defects in graphene via raman spectroscopy at different excitation energies. *Nano letters*, 11(8):3190–3196, 2011.

[14] Nick FW Thissen, RHJ Vervuurt, JJL Mulders, JW Weber, WMM Kessels, and AA Bol. The effect of residual gas scattering on ga ion beam patterning of graphene. *Applied Physics Letters*, 107(21):213101, 2015.

[15] Isaac Childres, Luis A Jauregui, Jifa Tian, and Yong P Chen. Effect of oxygen plasma etching on graphene studied using raman spectroscopy and electronic transport measurements. *New Journal of Physics*, 13(2):025008, 2011.

[16] S Vollebregt, B Alfano, F Ricciardella, AJM Giesbers, Y Grachova, HW van Zeijl, T Polichetti, and PM Sarro. A transfer-free wafer-scale cvd graphene fabrication process for mems/nems sensors. In *2016 IEEE 29th International Conference on Micro Electro Mechanical Systems (MEMS)*, pages 17–20. IEEE, 2016.

[17] Eldad Grady, Marcel Verheijen, Tahsin Faraz, Saurabh Karwal, W. M. M. Kessels, and Ageeth A. Bol. Tailored molybdenum carbide properties and graphitic nano layer formation by plasma and ion energy control during plasma enhanced ald, 2019.

[18] Eldad Grady, W. M. M. Kessels, and Ageeth A. Bol. Control of graphene layer thickness grown on plasma enhanced atomic layer deposition of molybdenum carbide, 2019.

[19] Rene HJ Vervuurt, Bora Karasulu, Marcel A Verheijen, Wilhelmus (Erwin) MM Kessels, and Ageeth A Bol. Uniform atomic layer deposition of al2o3 on graphene by reversible hydrogen plasma functionalization. *Chemistry of Materials*, 29(5):2090–2100, 2017.

Figures

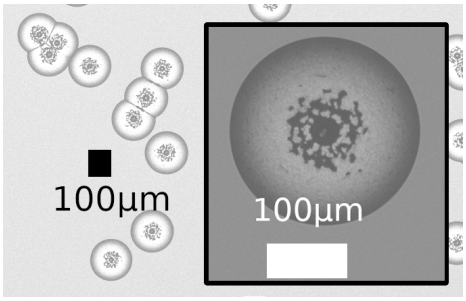

(a) SEM: MoC_x ablation

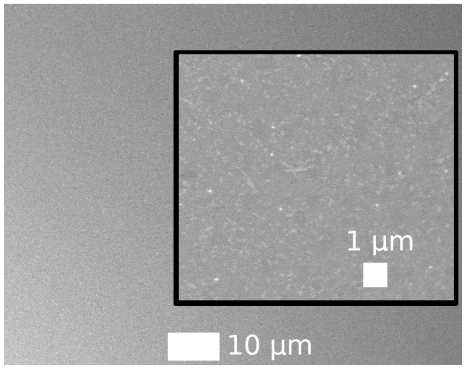

(b) SEM: MLG grown on MoC_x

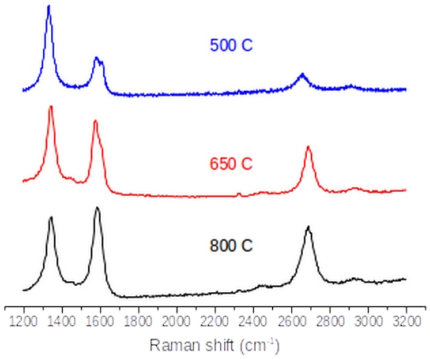

(c) Raman spectra (carb. temp)

Figure 1: SEM images and Raman spectrum of MoC_x after CH_4 annealing at $1100°C$. Top: (a) SEM image of films that were not carburised prior to growth. Bottom: (b) SEM image of MLG grown on carburised MoC_x film. Smooth surface no signs of inhomogeneity. (c) Raman spectrum after graphene growth, as a function of carburisation temperature. Growth time remained identical for all 3 experiments.

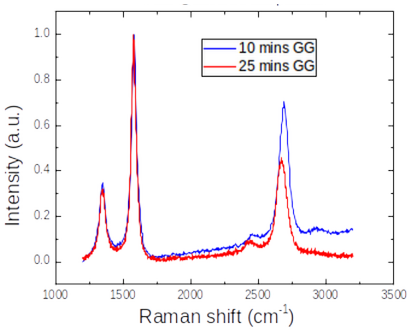

(a) Amorphous MoC_x

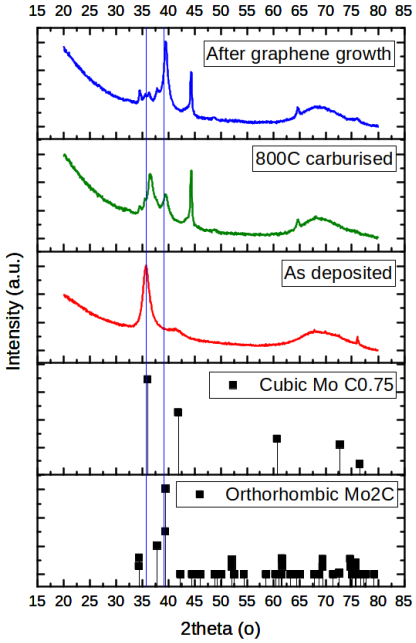

(b) XRD of crystalline MoC_x

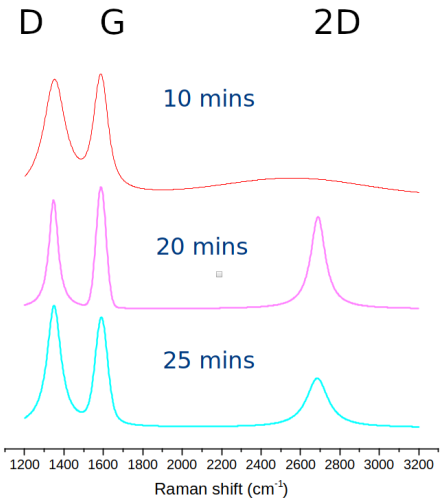

(c) Crystalline MoC_x

Figure 2: Raman spectra and XRD measurements. Top: Raman measurements of MLG grown on amorphous MoC_x film after 10 and 25 minutes growth at $1100°C$. Bottom: (b) XRD measurements of crystalline MoC_x for each step from ALD to graphene growth

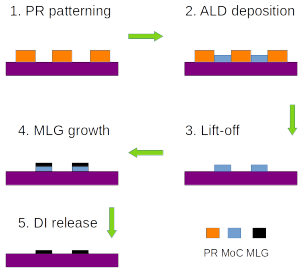

(a) Fabrication flow chart

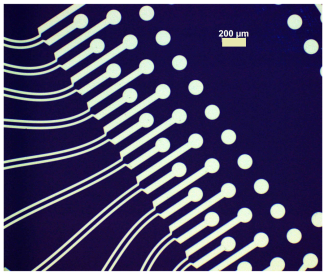

(b) Pre patterned MoC_x ALD

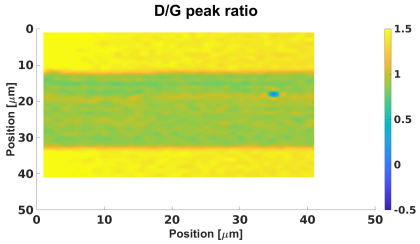

(c) D/G peak ratios mapping

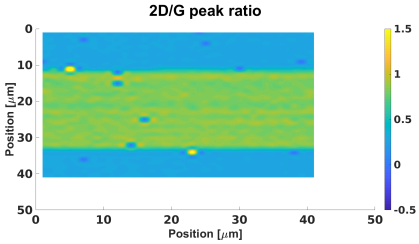

(d) 2D/G peak ratios mapping

Figure 3: Fabrication of patterned MLG. (a) Fabrication flow schematics. (b) Top right: optical microscopy of pre patterned MoC_x ALD at $50°C$ after deposition. Bottom: Raman mapping scan of $40\mu m$x$40\mu m$ area with $1\mu m$ step resolution of MLG grown on 20 μm thick MoC_x ALD film . (c) left: D/G peak ratio shows a high D/G peak ratio, albeit uniformal continuous coverage. (d) Right: 2D/G peak ratio show a uniform continuous MLG film. Variation in colour is inversely proportional to MLG uniformity

(a) Fabrication flow chart (b) PEALD on SiN membrane

Figure 4: Illustration of suspended heterostructure and optical images. Left (a) Fabrication schematics of suspended graphene heterostructure. (b) Right: Optical images of SiN membranes before and after PEALD of ~ 15 nm MoC_x film on top.

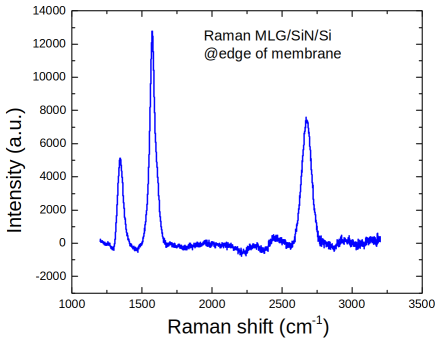

(a) MLG/SiN/Si substrate

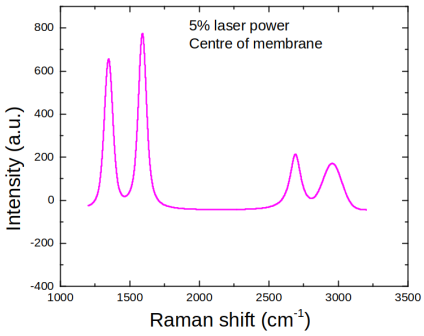

(b) suspended MLG/SiN membrane

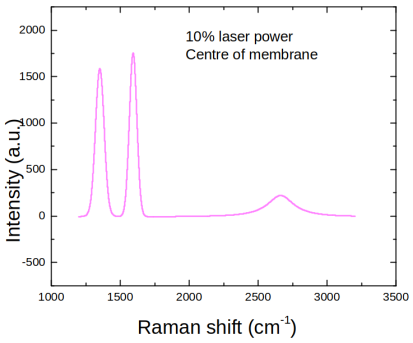

(c) Suspended MLG/SiN membrane

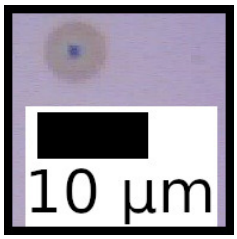

(d) Suspended MLG/SiN membrane

Figure 5: Raman spectrum of MLG on SiN membrane. Measurements taken on the membrane's edge with underlying Si, and at various spots around the centre of the membrane with increasing laser power. (a) MLG on SiN membrane's edge with underlying Si substrate. (b) Raman scan measured with 5% laser power shows diminished 2D peak and a rise in D peak. (c) Raman scan measured with 10% laser power shows quenched 2D peak and a high D peak. (d) Raman scan measured with 50% laser power punches a hole in the MLG/SiN suspended heterostructure